

Chapter 5

Tunable Magnetic Anisotropy and Magnetization Reversal in Microwires

A. Chizhik, A. Stupakiewicz, and J. Gonzalez

5.1 Introduction

Understanding the physical nature of magnetic microwires on a wide-frequency regime led to a novel technologies based on magnetic sensors. In developing of the sensor technology it is very important to possess sensitive methods for investigations and detections of the magnetization states. In magnetic materials the interplay of magnetism and optics led to a high sensitivity magneto-optical experimental method. Being of a sub-micrometer spatial resolution, it brings new and complementary information in comparison with classical magnetometry, partly due to the high sensitivity of the magnetic signal from the microwire surface. The microwire-based sensors usually operate on the giant magneto-impedance (GMI) effect. The GMI effect was discovered 20 years ago [1]. In soft magnetic materials, such as composite amorphous thin wires, the impedance change is in the range of more than 100 % in the high-frequency band for the low external magnetic fields of 0.1 mT [2]. The surface magnetic anisotropy in microwire is originated by the distribution of internal stress which depends on the thermal and the mechanical prehistory of a wire [3]. Another words, the real distribution of magnetic anisotropy in microwires is determined by the sign and value of the magnetostriction originated in turn by the stress distribution [4–9].

The task of the determination of the limit angle of the helical anisotropy induced by the torsion stress exists since 90 years [10, 11], when it was demonstrated that the torsion stress is a sum of tension perpendicular stresses, each acting at 45°

A. Chizhik (✉) • J. Gonzalez
Departamento Facultad de Quimica, Universidad del País Vasco UPV/EHU, San Sebastian,
Spain
e-mail: oleksandr.chyzyk@ehu.es

A. Stupakiewicz
Laboratory of Magnetism, Faculty of Physics, University of Bialystok, Bialystok, Poland

relative to the wire axis. The tensile stress is directed along one axis and while the opposite compressive stress is directed along another axis. The purpose of the present work is to demonstrate the limits of the torsion stress induced inclination of the helical anisotropy.

Taking into account that the GMI effect is based on the skin effect the circumferential permeability is essential for the observation of a high GMI effect in cylindrically shaped wires. The study of the formation and transformation of the surface magnetic structure in the presence of a high-frequency (HF) electric current is a fundamental task for the design of magnetic sensors. At the moment, the details of this transformation are under question. The temperature dependent behaviour of the domain structure (DS) in the microwire is also very important for stable sensor functioning. Considering the strong internal stresses arising from the difference in thermal expansion coefficients of glass and metallic alloy [2] we assumed that the surface magnetic structure should experience great transformation in a temperature range higher than room temperature.

The internal stress in microwires sufficiently affects the magnetization reversal process. In particular it limits the single domain wall (DW) propagation regime via the giant Barkhausen effect. Earlier we studied the single DW dynamics using magneto-optical Kerr effect (MOKE) modified Sixtus-Tonks method [12–14].

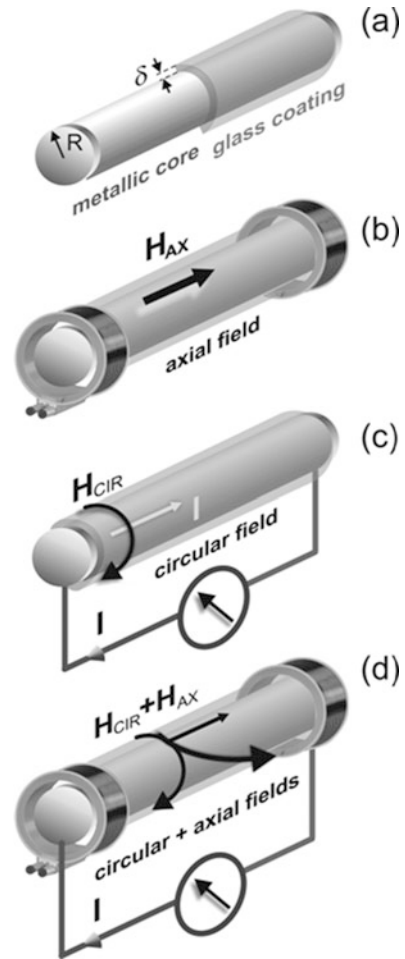
Recently, a number of studies of the DW motion in metallic microwires have used a Sixtus-Tonks method with a few pick-up magnetic coils to study the effect of the magnetoelastic anisotropy on the DW velocity [15] and the local DW nucleation [16] on a volume of the microwire. This technique does not present the direct visual observation of the DW dynamics. The MOKE microscopy permits a local observation of both the magnetic domain structures and the DW motion. In particular it allows analysis of the changing geometry of the DW under both circular and axial magnetic fields.

The present chapter consists of four parts: (1) “Experimental details”—describes the MOKE method in different geometries adapted to the cylindrically shaped glass covered microwires; (2) “Mechanical torsion stress effect”—presents the experimental results of the stress induced transformation of the surface magnetic structure. The limit of induced helical anisotropy also considered; (3) “Temperature effect”—is dedicated to the variety of the surface domain structures and magnetization reversal caused by the temperature variation; (4) “High-frequency electrical current effect” is devoted to influence of high-frequency electric current and circular magnetic field on the mechanism of surface magnetization reversal.

5.2 Experimental Details

The different geometries of observation of the surface magnetic domain structures and magnetization reversal process in cylindrical microwires using MOKE have been demonstrated. The separation of the magnetization components in the wire

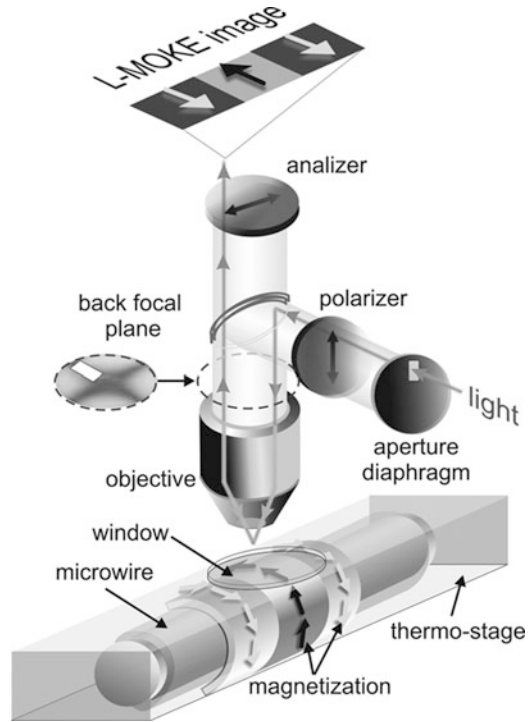
Fig. 5.1 The schematic configuration of the microwire (a), the orientation of the axial magnetic field (b), the orientation of the circular magnetic field (c), and the orientation by the helical direction of the field by the superposition of the orthogonally directed the circular and the axial magnetic fields



using vector magnetometry and analysis of both the hysteresis curves and the images of the magnetic domain structures were performed using these methods.

The investigations of the microwires (see Fig. 5.1a) were performed using MOKE microscopy with different configurations of the external magnetic field: (1) axial (H_{AX}), (2) circular (H_{CIR}), and (3) the sum $H_{CIR} + H_{AX}$. A pair of Helmholtz coils provided an external magnetic field, H_{AX} , with an axial orientation at the microwire (see Fig. 5.1b). To produce the H_{CIR} , an electric current was passed through the microwire (see Fig. 5.1c). In the static regime, the maximum amplitude of the current usually was <3 mA. At this value, the investigations were outside the regime that could induce over-heating. The circular magnetic field was calculated using the formula $H_{CIR} = I/(2\pi R)$ where I is the electric current flowing through the microwire. To produce the superposition of the orthogonally directed the circular

Fig. 5.2 The experimental L-MOKE configuration for the observation of the magnetic domain structures in microwires at different temperature and the schematic localization of the main components for observation back focal plane using aperture diaphragm. Design of the skin on microwire marked by the magnetization orientation



and the axial magnetic fields were applied to the microwire. In result we obtained the helical direction of the magnetic field with amplitude $H_{CIR} + H_{AX}$ (see Fig. 5.1d).

The surface magnetic domain structures in all microwire were investigated using a high-resolution, wide-field magneto-optical polarizing microscope working in reflective mode. The essential components of the microscope and a ray diagram are shown in Fig. 5.2. A high-sensitive camera has a fast-frame rate with a thermo-electrical cooling CCD chip was used. Digital images of 1344×1024 pixels were captured with an exposure time between 10 and 100 μ s. The spatial resolution of the images was estimated to be 300 nm. The aperture diaphragm was used to control the incident angles of the light rays that reached the surface of the microwire and also determined the MOKE geometry at the microscope [17]. The plane of the aperture diaphragm is conjugate to the back focal plane of the objective lens. When the polarizer and the analyzer were crossed, the cross-shaped image defined the extinction area (the conoscopical image) that was observed in this plane. For the L-MOKE geometry, a slit aperture was displaced from the centre and oriented both parallel to the plane of light incidence.

The initial optical images of the microwire were recorded using a microscope with focusing objective lens close to the top metallic surface of the wire. In a microwire that has helical magnetic anisotropy, we can observe both circular and axial components of the magnetization under the external axial magnetic field,

H_{AX} . The visualization of the magnetic domain structure in the microwire was performed in both the P-MOKE and the L-MOKE geometries with out-of-plane and in-plane magnetization sensitivity, respectively [18].

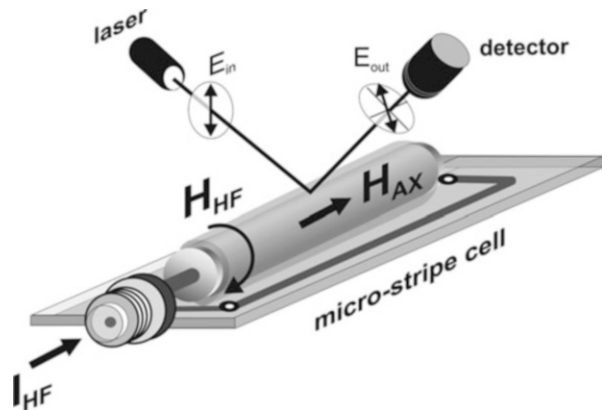
For our investigations we use mainly the L-MOKE configuration. The contrast in images of domain structures shows the difference between the in-plane magnetization components. The movement of the non-central position of the hole in aperture diaphragm (Fig. 5.2) leads to a change in the orientation of the plane of incidence of the light along the perpendicular or the parallel direction to the axial direction of the wire.

In the case where the direction of incidence was parallel to axial orientation of the wire, we observed the maximum magnetic contrast at the domains where the magnetization was in the direction of the wire. In the second case, when the direction of incidence was perpendicular to the axial orientation of the wire, the contrast at the domains in the axial direction of the magnetization decreased. The contrast of the domains with circular-only directions of the magnetization (that were perpendicular to the axial orientation) increased. Each of the in-plane magnetization components in the microwire was non-zero.

For the registration of the surface magnetic domains, we used the standard procedure that was developed to get contrast in the magnetic domains by subtracting the average images. The sample was initially saturated with relatively large amplitude of the magnetic field. When the mono-domain state appeared with this applied field, the image was recorded as the reference image. At the same time, the reference image was subtracted from next image, at the same saturation field. In the next step, the images were processed in real time while continuously varying magnetic field. Each image was the result of the difference between the image of the domain structure in a given external magnetic field and the reference image. It is significant that the “black and white” contrast on image of domain structure corresponds to the in-plane component of the magnetization (see Fig. 5.2).

The temperature change of magnetic domain structures in microwires was performed by means of MOKE microscope with a thermo-controlled system (see Fig. 5.3). This system consists of a thermo-stage and system controller operated

Fig. 5.3 Micro-strip cell used to MOKE study in the presence of a high-frequency electric current I_{HF}



within -0 to 300 °C temperature range. To observation of images of magnetic domain structure was used the same procedure of image processing.

To magnetization reversal process was studied using the MOKE magnetometer, where the L-MOKE and transversal (T-MOKE) configurations were employed. For the L-MOKE configuration, the rotation of the plane of the polarization of the light, reflected from the surface of microwire, is proportional to the axial component of the magnetization. For the T-MOKE configuration, the intensity of the reflected light is proportional to the magnetization, which is perpendicular to the plane of the light (circular projection of the magnetization). The details of the T-MOKE experimental setup have been presented elsewhere [18].

A polarized light from the He-Ne laser was reflected from the surface of the wire to the detector. The beam diameter was of 0.8 mm. For the transverse Kerr effect, the intensity of the reflected light is proportional to the magnetization oriented perpendicularly to the plane of the light polarization (the plane which contains the laser beam and the microwire). In the present experiments, the circular magnetization is the magnetization, which is perpendicular to the plane of the light polarization. Therefore, the light intensity is proportional to the circular projection of the magnetization in the surface area of the wire.

To apply the high-frequency (HF) electric current in the MHz–GHz band, the microwire was soldered in a specially designed micro-strip cell (Fig. 5.3). The HF current flows through the wire. This cell is usually used in GMI experiments.

5.3 Mechanical Torsion Stress Effect

Generally, the influence of the torsion stress on the coercive properties or magneto-impedance could be presented in the form of dependence on the value of the torsion angle [10, 11, 19]. Here we demonstrate the direct correlation between the torsion stress and the helical magnetic anisotropy [20]. Physically more informative the experimental results could be presented as a dependence on the helical anisotropy. Torsion stress induced limit of the angle of helical anisotropy has been theoretically shown earlier, but the experimental demonstration of this limit has not been demonstrated. Here we demonstrate experimentally the limits of the helical anisotropy induced by the torsion stress. The MOKE experiments have been performed in amorphous microwires of nominal composition $\text{Co}_{69.5}\text{Fe}_{3.9}\text{Ni}_1\text{B}_{11.8}\text{Si}_{10.8}\text{Mo}_2$ (metallic nucleus radius was 9.5 μm , glass coating thickness was 2.6 μm) supplied by TAMAG Iberica S.L.

The external torsion stress induces the transformation of the MOKE hysteresis loops (Fig. 5.4). We observe stress induced change of the amplitude and the sign of the jump of the MOKE intensity ΔI (another words, the circular magnetization ΔM_{CIR}). For example, for the stress of -2.2π rad m^{-1} (Fig. 5.4b) there is no jump of ΔM_{CIR} . The application of high enough negative stress (-22π rad m^{-1}) causes the appearance of the jump circular magnetization of the opposite sign (Fig. 5.4a).

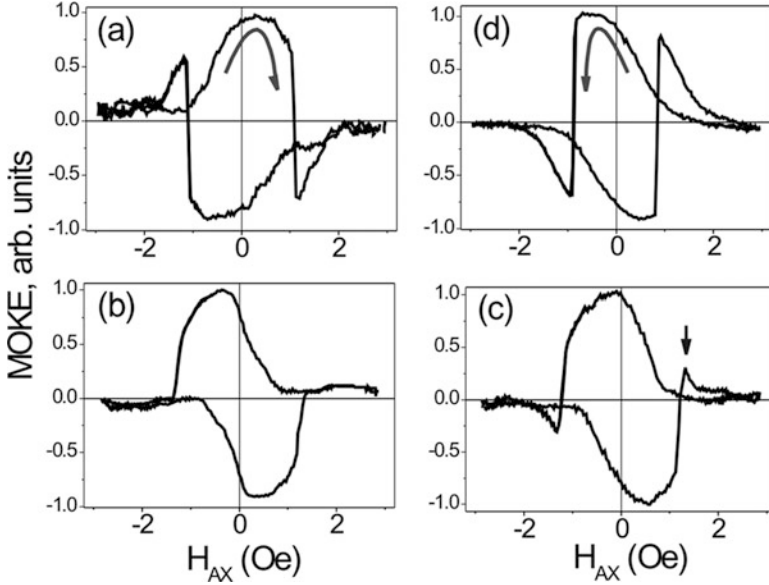


Fig. 5.4 T-MOKE dependencies in the presence of torsion stress: (a) $\tau = -22\pi \text{ rad m}^{-1}$, (b) $\tau = -2.2\pi \text{ rad m}^{-1}$, (c) $\tau = 0$, (d) $\tau = 8.9\pi \text{ rad m}^{-1}$. Reprinted with permission from [20] Chizhik, A., Zhukov, A., Blanco, J.M., Gonzalez, J., Gawronski, P.: *J. Magn. Magn. Mater.* 321, 803–805 (2009)

This transformation reflects the change of the surface helical anisotropy induced by the torsion stress.

Figure 5.5 demonstrates schematically the change of the surface helical anisotropy associated with the obtained MOKE experimental results. The normalized MOKE intensity is proportional to the normalized circular magnetization in the surface of the wire, i.e., $\Delta I/I_{\text{MAX}} \sim \Delta M_{\text{CIR}}/M_{\text{MAX}}$ (M_{MAX} is the maximal value of the circular magnetization during the surface magnetization reversal, I_{MAX} is the maximal intensity of the MOKE signal during the magnetization reversal). In Fig. 5.6 we can see the experimentally obtained normalized value of the jump of the MOKE intensity $\Delta I/I_{\text{MAX}}$ as a dependence on the external torsion stress. Knowing the jump of the circular magnetization we could determine experimentally the angle of helical anisotropy and establish the correlation between the surface hysteresis loop and this angle.

The calculation of the hysteresis loops has been performed taking into account that the helical magnetic anisotropy exists in the surface (outer shell) of the wire. While the curvature of the area of wire surface from which the light is reflected is about one angular degree, we consider in our calculations that the wire surface is a two-dimensional system. The external magnetic field H is a superposition of two orthogonal fields (H_{AX} and H_{CIR}), see Fig. 5.1d. The surface anisotropy changes the direction from axial to circular one. The energy of the system could be expressed as

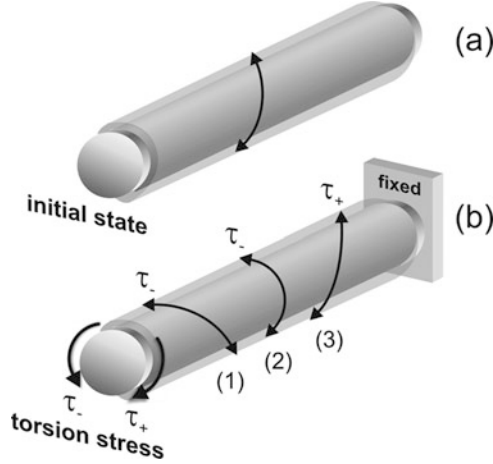
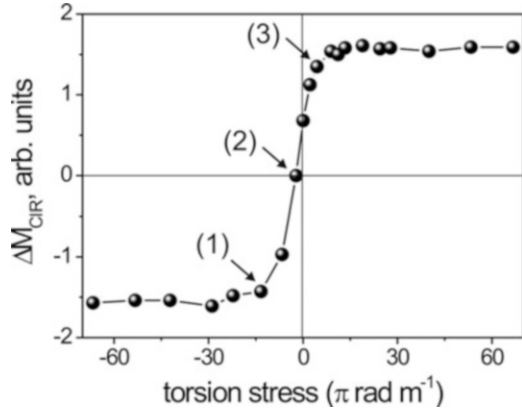


Fig. 5.5 Schematically pictures of the inclination of the axis of helical anisotropy induced by the torsion stress τ . The initial state of the microwire without stress (a) and alter right-hand τ_+ and left-hand τ_- torsion stress (b). The states (1, 2, 3) correspond to the magnetization states with helical component. Reprinted with permission from [20] Chizhik, A., Zhukov, A., Blanco, J.M., Gonzalez, J., Gawronski, P.: J. Magn. Magn. Mater. 321, 803–805 (2009)

Fig. 5.6 Experimental dependence of the normalized value of the jump of the Kerr intensity $\Delta I/I_{MAX}$ on applied torsion stress. Reprinted with permission from [20] Chizhik, A., Zhukov, A., Blanco, J.M., Gonzalez, J., Gawronski, P.: J. Magn. Magn. Mater. 321, 803–805 (2009)



$$\begin{aligned}
 U &= -K_U \cos^2(\theta - \varphi) - H \cdot M \\
 &= -K_U \cos^2(\theta - \varphi) - H_{AX} \cos(\theta) - H_{CIR} \sin(\theta)
 \end{aligned}
 \tag{5.1}$$

where K_U is uniaxial anisotropy constant, M is the saturation magnetization, φ is an angle between the anisotropy axis and the wire axis, and θ is the angle between the magnetic moment and the wire axis.

The numerical calculation was done by the coherent rotation approach [21]. The hysteresis loops were computed by the minimization of the energy term described by Eq. (5.1). For given values of the angle φ the minimization procedure can be

Fig. 5.7 Calculated dependence of the jump of the circular magnetization $\Delta M_{\text{CIR}}/M_{\text{MAX}}$ on the angle of helical anisotropy φ . Reprinted with permission from [20] Chizhik, A., Zhukov, A., Blanco, J.M., Gonzalez, J., Gawronski, P.: *J. Magn. Magn. Mater.* 321, 803–805 (2009)

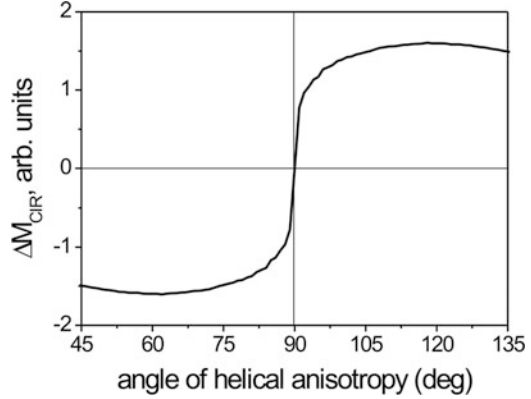
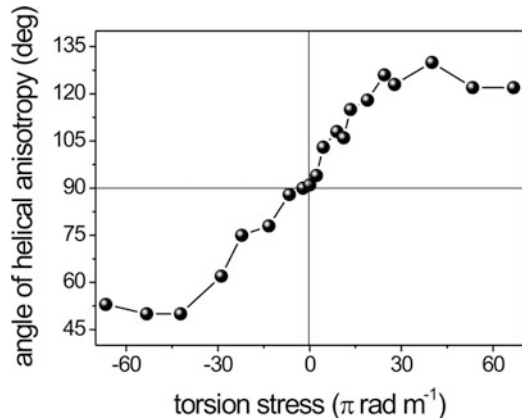


Fig. 5.8 Dependence of angle of helical anisotropy on applied torsion stress. Reprinted with permission from [20] Chizhik, A., Zhukov, A., Blanco, J.M., Gonzalez, J., Gawronski, P.: *J. Magn. Magn. Mater.* 321, 803–805 (2009)



outlined in the following way: each time the value of the axial field was changed, the search of the value of the angle θ that gave the minimal value of the energy term (Eq. (5.1)) was done.

The strong dependence of the jump of the circular magnetization on the angle of the helical anisotropy has been obtained as a result of the calculations. In Fig. 5.7 we present the calculated dependence of the $\Delta M_{\text{CIR}}/M_{\text{MAX}}$ on the angle of the helical anisotropy. When the magnetization is directed transversally the jump is equal zero. Two maximum for the values of the angle of 62° and 118° are observed in the calculated dependence.

Figure 5.8 is the result of the comparative analysis of the MOKE experiment (Fig. 5.6) and the calculations (Fig. 5.7).

There is a dependence of the angle of the helical anisotropy on the applied torsion stress. The surface anisotropy is directed almost to the transverse direction when the applied stress is absent. We have to mention that the small peak marked by arrow in Fig. 5.4c, means the small jump of circular magnetization. Therefore,

the angle of helical anisotropy is not exactly 90° . The application of stress of relatively small value of $-2.2\pi \text{ rad m}^{-1}$ causes the disappearance of this small peak. Thus, at this value of the torsion stress the surface anisotropy has a transversal direction. The angle of the helical anisotropy increases when the external stress increases. This growth finishes at the applied stress of the value of about $\pm 40\pi \text{ rad m}^{-1}$. Therefore, in such a way we confirm the prediction [10, 11] that the torsion stress induced inclination of the helical anisotropy does have a natural limit of 45° from the transverse direction independently on the value of the applied stress.

5.4 Temperature Effect

We studied Fe- and Co-based glass-coated amorphous microwires with different compositions: (1) $\text{Fe}_{71.7}\text{B}_{13.4}\text{Si}_{11}\text{Nb}_3\text{Ni}_{0.9}$ (metallic nucleus radius was $50 \mu\text{m}$, glass coating thickness was $20 \mu\text{m}$), (2) $\text{Fe}_{3.5}\text{Co}_{69}\text{B}_{15}\text{Si}_{10}$ (metallic nucleus radius was $37 \mu\text{m}$, glass coating thickness was $4 \mu\text{m}$), (3) $\text{Fe}_{5.71}\text{Co}_{64.04}\text{B}_{15.88}\text{Si}_{10.94}\text{Cr}_{3.40}\text{Ni}_{0.03}$ (metallic nucleus radius was $50 \mu\text{m}$, glass coating thickness was $20 \mu\text{m}$). MOKE hysteresis loops were obtained from the Kerr intensity for different H_{AX} as a result of the images processing. The hysteresis curves reflect the transformation of surface magnetization in the axial magnetic field [18]. Observing the temperature induced transformations in the magnetic structure we have extracted the common properties and the specific features of every studied microwires. The MOKE hysteresis loops of three studied wires consist generally of two parts: (1) the part of coherent rotation of magnetization and (2) the switching magnetization part. The second part is determined by the transformation of the domain structure associated with the domain structure rearrangement or quick domain walls motion.

First we have studied the $\text{Fe}_{3.5}\text{Co}_{69}\text{B}_{15}\text{Si}_{10}$ microwire. Figure 5.9 presents the transformation of the MOKE hysteresis curves. The hysteresis loop consists of the

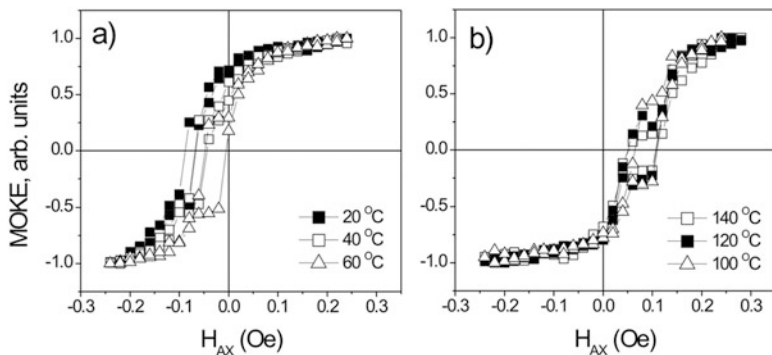


Fig. 5.9 $\text{Fe}_{3.5}\text{Co}_{69}\text{B}_{15}\text{Si}_{10}$ microwire. MOKE hysteresis loops obtained in the presence of an H_{AX} at different temperature: (a) 20°C , 40°C , and 60°C ; (b) 100°C , 120°C , and 140°C

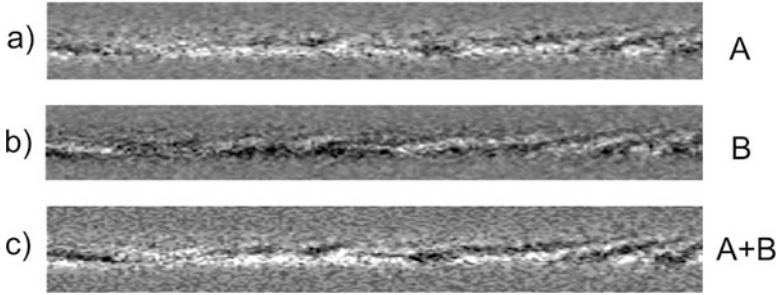


Fig. 5.10 The images of domain structures obtained at 20 °C: (a) $H_{AX} = -0.08$ Oe; (b) $H_{AX} = -0.1$ Oe. (c) result of the digital sum of (a) and (b). The size of images is $400 \mu\text{m} \times 55 \mu\text{m}$

fluent and sharp parts within the temperature range of 20–140 °C. The sharp jumps changes with the temperature increase. The noticeable shift of the Kerr loops along the axis of H_{AX} (see Fig. 5.9) was fixed as an influence of the temperature.

Generally, as it was found earlier, *dc* circular magnetic field could be the reason of such type of hysteresis shifts, but we have not applied the circular field in our present experiments. Another possible reason of the directed shift is the surface helical anisotropy. From the value of this shift we determine the type of the surface domain structures. As it was found earlier [22], this shift reflects the surface magnetic helicality and the degree of helical structure could be extracted from it. Therefore, change of the angle of the surface helical structure induced by the temperature change takes place in the present experiment. The crossing of the “0” value of the axial magnetic field corresponds to the helical anisotropy of 90°. This configuration means the pure circular magnetic state.

Images presented in Figs. 5.10a, b have been obtained in short range of the external magnetic field containing the jump of the magnetization demonstrated in Fig. 5.9. Figure 5.10a, b differs only in the contrast of the domains—the black colour was changed to the white colour and vice versa. We have supposed that the domain walls have not moved during this jump. To verify this supposition we have produced the digital sum (Fig. 5.10c) of images (a) and (b). The resulting image confirms the suggestion: repeats the original domain configuration. It means that the quick jumps in the hysteresis loop are related to the transformation of the surface magnetic structure without the domain walls movement.

Figure 5.11 demonstrates the transformation of the Kerr hysteresis obtained in $\text{Fe}_{71.7}\text{B}_{13.4}\text{Si}_{11}\text{Nb}_3\text{Ni}_{0.9}$ microwire. The hysteresis loop consists of fluent rotation of the magnetization and jumps of the circular magnetization. The jump decreases with temperature disappears completely at 50 °C (Fig. 5.10b).

In differece with the $\text{Fe}_{3.5}\text{Co}_{69}\text{B}_{15}\text{Si}_{10}$ microwire, here we have fixed the quick motion of the domain walls (Fig. 5.12). The surface domain structure consists of two types of domain structures (type I and type II). They have different period of domain structure and different angle of the domain walls inclination relatively circular direction. The domain structure of the type I (central part of the image in Fig. 5.12) contains a DW with high mobility. The jumps of the Kerr signal are

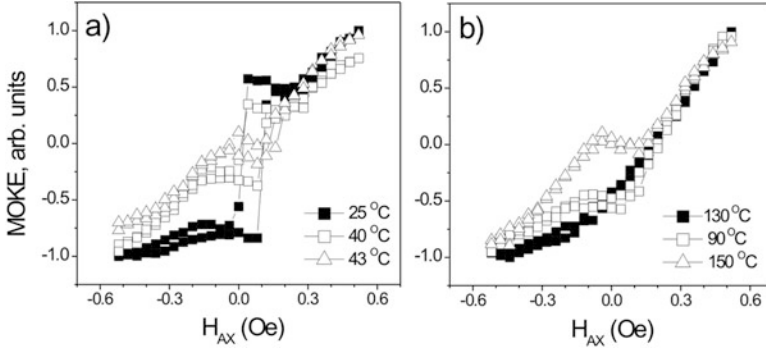


Fig. 5.11 $\text{Fe}_{71.7}\text{B}_{13.4}\text{Si}_{11}\text{Nb}_3\text{Ni}_{0.9}$ microwire. MOKE hysteresis loops obtained in the presence of an H_{AX} at different temperatures: (a) 25 °C, 40 °C, and 43 °C; (b) 50 °C, 90 °C, and 130 °C

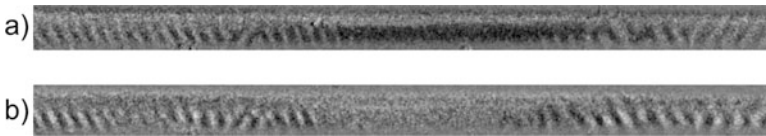


Fig. 5.12 The images of domain structures obtained at 40 °C: (a) $H_{\text{AX}} = -0.5$ Oe; (b) $H_{\text{AX}} = 0.12$ Oe. The size of images is $600 \mu\text{m} \times 40 \mu\text{m}$

related to the quick motion of the solitary DW. The switching of the angle of the inclination is the characteristic feature of the structure II.

Figure 5.12a, b demonstrates the domain structures before and after the jump of the solitary domain wall realized in the domain structure I. Periodic domains are the samples of the structure II. Generally, structure II has helically inclined domains with two opposite directions of the inclination.

At the temperature of 50 °C the domain structure of I type disappears. This disappearance is correlated with the disappearance of the minor rectangular loop in the MOKE hysteresis (Fig. 5.11b).

It is evident that we have experimentally found coexistence of four helically oriented states which have been theoretically predicted in our paper [23]. The multi-domains structure observed in this microwire is related to the internal stresses distribution inside the microwire. Because of difference between the thermal expansion coefficients of glass coating and metallic nucleus the glass coating introduces mentioned stresses [2]. Due to the magnetoelastic coupling between magnetization and internal stresses through magnetostriction, the internal stresses are the source of the magnetic anisotropy. These internal stresses are originated by high quenching rate and solidification process during the wire fabrication. The solidification usually proceeds from the wire surface causing the distribution of stresses along the wire depth.

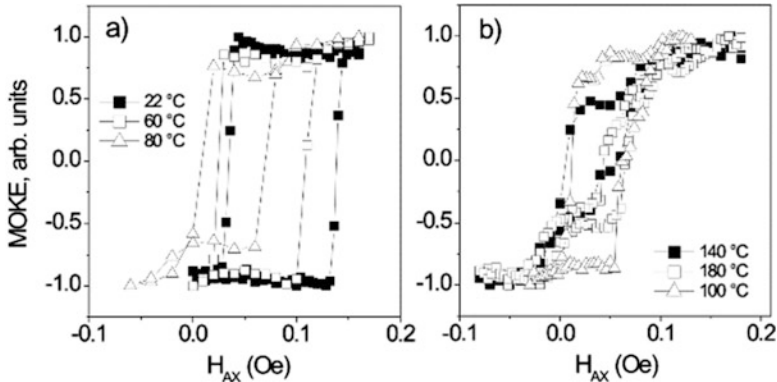


Fig. 5.13 $\text{Fe}_{5.71}\text{Co}_{64.04}\text{B}_{15.88}\text{Si}_{10.94}\text{Cr}_{3.40}\text{Ni}_{0.03}$ microwire. MOKE hysteresis loops obtained in the presence of H_{AX} at different temperatures: (a) 22 °C, 60 °C, 80 °C; (b) 100 °C, 140 °C, and 180 °C

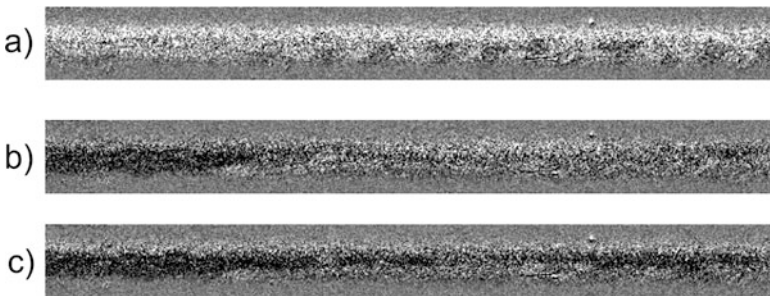


Fig. 5.14 The images of domain structures obtained at 100 °C: (a) $H_{\text{AX}} = 0.05$ Oe, (b) $H_{\text{AX}} = 0.07$ Oe, (c) $H_{\text{AX}} = 0.08$ Oe. The size of images is $500 \mu\text{m} \times 50 \mu\text{m}$

The $\text{Fe}_{5.71}\text{Co}_{64.04}\text{B}_{15.88}\text{Si}_{10.94}\text{Cr}_{3.40}\text{Ni}_{0.03}$ microwire has rectangular hysteresis between the room temperature and 60 °C. This rectangularity means the existence of the effect of the circular bistability in this wire [24] (Fig. 5.13a). The heating process causes the transformation of the surface magnetic structure which is reflected in the hysteresis loop. The value of the jumps decreases with the temperature.

At high temperatures two types of domain structures have been found in this wire. The quick motion of the domain wall of type I is covered by the un-moved domains of type II. To demonstrate pure motion of the solitary domain wall we have performed the following image treatment. First, we have fixed the magnetic structure containing the small domains of the type II (Fig. 5.14a). Second step, we have used this image as a reference. Based on this reference image we have demonstrated the motion of the solitary domain wall (Fig. 5.14b, c). At the final part of the surface magnetization reversal the domains of the type II were observed again.

We consider that the temperature influence on the magnetic surface properties is stronger for the wire with the positive magnetostriction constant of 20×10^{-6} . It is related to the special magnetic structure of this wire: axially magnetized inner core, radially magnetized outer shell, and the helically magnetized surface closure domain structure. The coexistence of two types of surface domain structure takes place in very short temperature range. Two other magnetic microwires have basically helical magnetic structure with some distribution of the helicity. This structure is more homogeneous. Therefore, the temperature transformation of domain structures in these wires is weaker.

5.5 High-Frequency Electric Current Effect

The specially designed micro-strip cell has been used to apply the HF electric current I_{HF} in the MHz–GHz band (see Fig. 5.3). Usually this cell is used for GMI experiments [25].

Figures 5.15 and 5.16 present the MOKE hysteresis curves obtained in the presence of HF electric current of the MHz range. Figure 5.17 shows schematically the mechanisms of the surface magnetization reversal. The strong transformation of the hysteresis loop is observed that reflects the transformation of the magnetization reversal process. For the small value of the circular magnetic field ($I_{\text{HF}} = 2$ mA, Fig. 5.15) the hysteresis consists of the domain structure transformation and rotation of the magnetization in the surface (Fig. 5.17b). The electric current of 2 mA corresponds to the circular magnetic field of 0.35 Oe. An increase of the HF circular magnetic field (I_{HF} up to 10 mA) induces an asymmetric transformation of hysteresis loop. The following increase of the circular magnetic field amplitude (I_{HF} up to 20 mA) induces a change of the re-magnetization mechanism—the rotation of the magnetization dominates (Fig. 5.17a). We have to remark that this mechanism

Fig. 5.15 MOKE hysteresis loops in the presence of an HF electric current with 1 MHz frequency and varying amplitude of the current

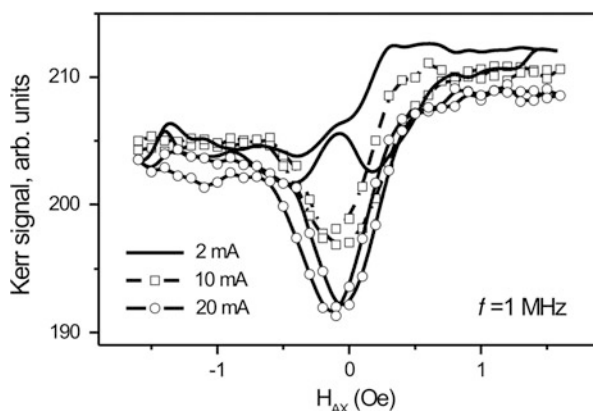


Fig. 5.16 MOKE hysteresis loops in the presence of an HF electric current. Comparison hysteresis loops in the presence of 1 MHz and 300 MHz frequency current

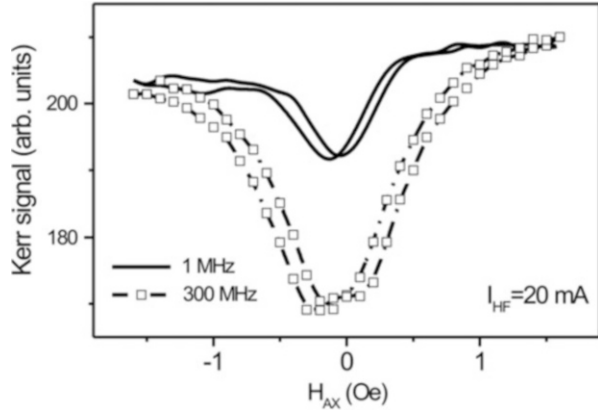
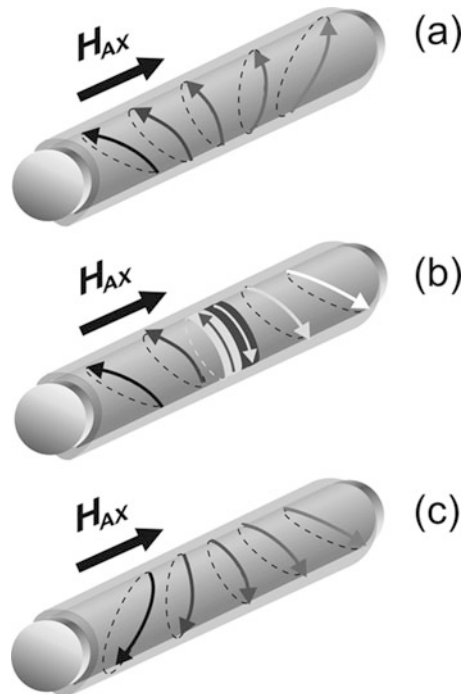


Fig. 5.17 Schematic pictures demonstrated mechanisms of the surface magnetization reversal under axial magnetic field H_{AX} . The arrows schematically show the magnetization orientations



of the magnetization reversal is completely different from the magnetization reversal observed earlier in the presence of *dc* circular magnetic field [23].

To clear more deeply the details of the mechanism of the magnetization reversal, we have performed the following experiment. The MOKE hysteresis loops have been obtained in the presence of the HF electric current of the constant amplitude (20 mA). The frequency was changed in the band of 0.1–3 GHz (Fig. 5.18). The shape of the presented curves could be interpreted in the following way: the HF

Fig. 5.18 MOKE hysteresis loops obtained in the presence of an HF electric current of 20 mA for the different frequencies

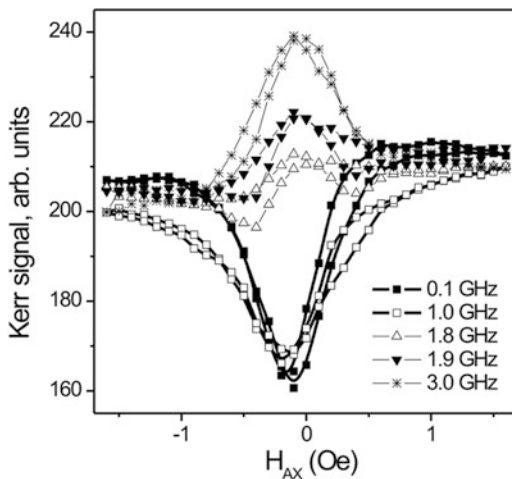
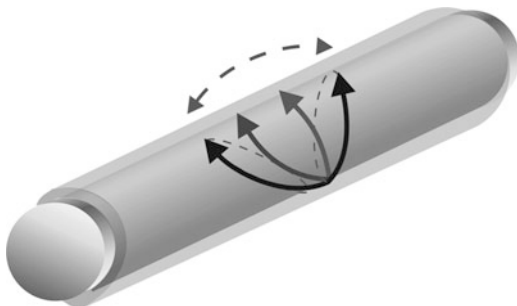


Fig. 5.19 Schematic of the magnetization vibration on the surface of the microwire



circular magnetic field causes such type of the energetic distribution that one of the surface circular phases is in an advantageous state, and the rotation of the magnetization in this domain is observed (Fig. 5.17a). The change of the frequency from 0.1 to 1 GHz only accelerates the rotation of the magnetization without changing of the essential of the mechanism. In this way, the circular field of 1 GHz causes a greater inclination of the circular magnetization from the axial direction than the circular field of 0.1 GHz.

Increasing the frequency we have found an unexpected effect. For the short band of the frequency (1.8–1.9 GHz) a strong transformation of the hysteresis loop takes place. For the frequency of 1.8 GHz, the MOKE hysteresis loop contains the regions which are interpreted as a clear rearrangement of the surface domain structure. For the frequency of 1.9 GHz, the opposite circular domain is the advantageous one and we observed coherent rotation of the magnetization in the surface of the wire. We explain this effect by the existence of a small initial helical anisotropy which exists originally in the studied wire (Fig. 5.19). Obviously, HF field induces an increase of the vibration of the magnetization. The meta-stable advantageous domain changes its sign to the opposite one when the vibrating helical magnetization overcomes the axial direction of the microwire.

For the frequency of 3 GHz, a pure rotation of the magnetization is also observed. The magnetic field of 3 GHz causes the following transformation: the meta-stable surface state becomes more inclined. The higher amplitude of the MOKE signal is the result of this effect of inclination. Generally, this effect finds the interpretation in the context of low field absorption and splitting between the ferromagnetic resonance and GMI effect [26].

We consider that the surface magnetic structure is the result of the superposition of the orthogonally directed HF circular and *dc* axial magnetic fields. The amplitude of the magnetic field generated by the exiting current of 20 mA is about 3.5 Oe in the wire surface that is higher than the quasi-static field applied in our experiments (about 2 Oe), while it is of the same order as the value of the static field applied typically in GMI experiments for such type of microwire [27, 28]. Following [29] we assume that for the high value of the HF circular field a microwave response of microwire is mainly associated with the inhomogeneous surface excitations of the magnetization vector. The *dc* axial field is smaller than the HF circular field, but it is high enough to incline the equilibrium direction of helical magnetization relatively which the surface magnetization vibrates. The actual mechanism of the surface magnetization reversal is determined basically by the existence of four helical structures revealed earlier in [23]. The dynamic superposition of the two fields leads to the periodical change of the helical configuration. For the frequency of 1.9 GHz this change occurs as a magnetization switching.

5.6 Conclusion

The transformation of surface magnetic structures and magnetization reversal process have been studied in the Co- and Fe-rich amorphous microwires in the presence of the torsion stress, the temperature, and high-frequency electric current.

The analysis of the torsion stress induced transformation of hysteresis loops and domain structures has permitted us to establish the direct correlation between the angle of helical magnetic anisotropy and the value of the torsion stress. The real limit of the angle of the helical anisotropy has been determined. The earlier predicted value of 45° has been confirmed experimentally. Now we have an original method to present the results of the experiments with torsion stress as a dependence on the angle of helical anisotropy.

Taking into account the importance of circumferential permeability, we focus on the formation and the transformation of different types of magnetic domain structures induced by the HF circular magnetic field and the temperature.

The general regularities of the heating induced transformation of surface magnetization reversal and domain structure have been established. We have found that the surface magnetization reversal consists of the coherent rotation of the magnetization and the surface domain structure changes. In some microwires the quick directed solitary domain wall motion was observed while in other wires the rearrangement of domain structure rearranges in regular or irregular manner. The

quick jump in the MOKE hysteresis related to the domain wall motion disappears with temperature decrease. Another word, the heating suppresses the coexistence of two types of surface domain structures. The interplay of surface and internal mechanical stresses originated by the microwires fabrication process is the main reason of the domain structure transformation.

One of the observed essential effects in the presence of a low HF circular field is the sharp change in the direction of the magnetization in the existing domains. The contribution of this type of magnetization reversal is very essential to the circumferential permeability and, in turn, to the GMI amplitude. Also we have found that the HF circular magnetic field induces the existence of meta-stable inclined helical states. The sign of the inclined state and the degree of the helicity depend on the frequency and the amplitude of the HF magnetic field.

The temperature induced rearrangement of surface magnetic domain structure is examined in frame of providing the stable operation of the GMI device. It has been observed experimentally the coexistence of surface domain structures with different values of domain wall mobility. It has an ambivalent influence on the GMI effect. The increase of the number of inclined domain walls with temperature causes an increase of the GMI effect. In turn, it leads to an increase of the sensor sensitivity. On the other hand, a change in the number of domain walls causes evidently the instability of the magnetic sensor operation.

Acknowledgements This work was supported by Spanish Ministry of Economy and Competitiveness (MINECO) under Project No. MAT2013-47231-C2-1-P, the Basque Government under Saitek 13 PROMAGMI (S-PE13UN014) and DURADMAG (S-PE13UN007) projects. A.C. acknowledges the financial support of Program of Mobility of the Investigating Personnel Basque Government MV-2015-1-15.

References

1. Panina, L.V., Mohri, K.: Magneto-impedance effect in amorphous wires. *Appl. Phys. Lett.* **65**, 1189–1191 (1994)
2. Zhukov, A., Zhukova, V.: *Magnetic Properties and Applications of Ferromagnetic Microwires with Amorphous and Nanocrystalline Structure*. Nova Science Publishers, New York (2009)
3. Chiriac, H., Ovari, T.A.: Switching field calculations in amorphous microwires with positive magnetostriction. *J. Magn. Magn. Mater.* **249**, 141–145 (2002)
4. Buznikov, N.A., Antonov, A.S., Granovsky, A.B.: Asymmetric magnetoimpedance in amorphous microwires due to bias current: effect of torsional stress. *J. Magn. Magn. Mater.* **355**, 289–294 (2014)
5. Xing, D., Chen, D., Liu, F., Liu, J., Shen, H., Ning, Z., Cao, F., SunT, J.: Torsion dependence of domain transition and MI effect of melt-extracted $\text{Co}_{68.15}\text{Fe}_{4.35}\text{Si}_{2.25}\text{B}_{13.25}\text{Nb}_1\text{Cu}_1$ microwires. *Adv. Mater. Sci. Eng.* **2015**, 1–6 (2015)
6. Gonzalez, J., Chen, I.P., Blanco, J.M., Zhukov, A.: Effect of applied mechanical stresses on the impedance response in amorphous microwires with vanishing magnetostriction. *Phys. Status Solidi A.* **189**, 599–608 (2002)
7. Phan, A.H., Yua, S.C., Kim, C.G., Vazquez, M.: Origin of asymmetrical magnetoimpedance in a Co-based amorphous microwire due to dc bias current. *Appl. Phys. Lett.* **83**, 2871–2873 (2003)

8. Betancourt, I.: Magnetization dynamics of amorphous ribbons and wires studied by inductance spectroscopy. *Materials*. **4**, 37–54 (2011)
9. Betancourt, I., Hrkac, G., Schrefl, T.: Micromagnetic study of magnetic domain structure and magnetization reversal in amorphous wires with circular anisotropy. *J. Magn. Magn. Mater.* **323**, 1134–1139 (2011)
10. Sablik, M.J., Jiles, D.C.: A modified Stoner-Wohlfarth computational model for hysteretic magnetic properties in a ferromagnetic composite rod under torsion. *J. Phys. D: Appl. Phys.* **32**, 1971–1983 (1999)
11. Sablik, M.J., Jiles, D.C.: Modeling the effects of torsional stress on hysteretic magnetization. *IEEE Trans. Magn.* **35**, 498–504 (1999)
12. Sixtus, K.J., Tonks, L.: Propagation of large Barkhausen discontinuities. *Phys. Rev.* **42**, 419 (1932)
13. Chizhik, A., Stupakiewicz, A., Maziewski, A., Zhukov, A., Gonzalez, J., Blanco, J.M.: Direct observation of giant Barkhausen jumps in magnetic microwires. *Appl. Phys. Lett.* **97**, 012502 (2010)
14. Chizhik, A., Zablotskii, V., Stupakiewicz, A., Dejneka, A., Polyakova, T., Tekielak, M., Maziewski, A., Zhukov, A., Gonzalez, J.: Circular domains nucleation in magnetic microwires. *Appl. Phys. Lett.* **102**, 202406 (2013)
15. Zhukov, A., Blanco, J.M., Ipatov, M., Chizhik, A., Zhukova, V.: Manipulation of domain wall dynamics in amorphous microwires through the magnetoelastic anisotropy. *Nanoscale Res. Lett.* **7**, 223 (2012)
16. Hudak, J., Blazek, J., Cverha, A., Gonda, P., Varga, R.: Improved Sixtus–Tonks method for sensing the domain wall propagation direction. *Sens. Actuators A*. **156**, 292–295 (2009)
17. Hubert, A., Schäfer, R.: *Magnetic Domains*. Springer, Berlin (1998)
18. Stupakiewicz, A., Chizhik, A., Tekielak, M., Zhukov, A., Gonzalez, J., Maziewski, A.: Direct imaging of the magnetization reversal in microwires using all-MOKE microscopy. *Rev. Sci. Instrum.* **85**, 103702 (2014)
19. Chizhik, A., Gonzalez, J., Zhukov, A., Blanco, J.M.: Magnetization reversal of Co-rich wires in circular magnetic field. *J. Appl. Phys.* **91**, 537–539 (2002)
20. Chizhik, A., Zhukov, A., Blanco, J.M., Gonzalez, J., Gawronski, P.: Experimental determination of limit angle of helical anisotropy in amorphous magnetic microwires. *J. Magn. Magn. Mater.* **321**, 803–805 (2009)
21. Bertotti, G.: *Hysteresis in Magnetism*. Academic Press, San Diego (1998)
22. Chizhik, A., Gonzalez, J.: *Magnetic Microwires: A Magneto-Optical Study*. Pan Stanford Publishing Pte. Ltd., Singapore (2014)
23. Chizhik, A., Zablotskii, V., Stupakiewicz, A., Gómez-Polo, C., Maziewski, A., Zhukov, A., Gonzalez, J., Blanco, J.M.: *Phys. Rev. B*. **82**, 212401–212404 (2010)
24. Chizhik, A., Gonzalez, J., Zhukov, A., Blanco, J.: Circular magnetic bistability in Co-rich amorphous microwires. *J. Phys. D: Appl. Phys.* **36**, 419–422 (2003)
25. Ipatov, M., Zhukova, V., Zhukov, A., Gonzalez, J., Zvezdin, A.: Low-field hysteresis in the magnetoimpedance of amorphous microwires. *Phys. Rev. B*. **81**, 134421 (2010)
26. Valenzuela, R., Zamorano, R., Alvarez, G., Gutiérrez, M.P., Montiel, H.: Magnetoimpedance, ferromagnetic resonance, and low field microwave absorption in amorphous ferromagnets. *J. Non-Cryst. Solids*. **353**, 768–772 (2007)
27. Zhukova, V., Chizhik, A., Zhukov, A., Torcunov, A., Larin, V., Gonzalez, J.: Optimization of giant magnetoimpedance in Co-rich amorphous microwires. *IEEE Trans. Magn.* **38**, 3090–3092 (2002)
28. Tousignant, M., Zabeida, M.O., Rudkowska, G., Yelon, A.: Investigation of surface effect on giant magnetoimpedance in microwires. *J. Magn. Magn. Mater.* **349**, 232–234 (2014)
29. Nakayama, K., Chiba, T., Tsukimoto, S., Yokoyama, Y., Shima, T., Yabukami, S.: Ferromagnetic resonance in soft-magnetic metallic glass nanowire and microwire. *J. Appl. Phys.* **105**, 202403 (2014)